Revista de metalurgia

Carburization of austenitic and ferritic alloys in hydrocarbon environments at high temperature

A. Serna* and R.A. Rapp**

Abstract

The technical and industrial aspects of high temperature corrosion of materials exposed to a variety of aggressive environments have significant importance. These environments include combustion product gases and hydrocarbon gases with low oxygen potentials and high carbon potentials. In the refinery and petrochemical industries, austenitic and ferritic alloys are usually used for tubes in fired furnaces. The temperature range for exposure of austenitic alloys is 800-1100 °C, and for ferritic alloys 500-700 °C, with carbon activities $a_c > 1$ in many cases. In both applications, the carburization process involves carbon (coke) deposition on the inner diameter, carbon absorption at the metal surface, diffusion of carbon inside the alloy, and precipitation and transformation of carbides to a depth increasing with service. The overall kinetics of the internal carburization are approximately parabolic, controlled by carbon diffusion and carbide precipitation. Ferritic alloys exhibit gross but uniform carburization while non-uniform intragranular and grain-boundary carburization is observed in austenitic alloys.

Keywords

Carburization. High temperature corrosion. Diffusion. Chromium molybdenum steels. Iron-chromium-nickel alloys.

Carburación de aleaciones austeníticas y ferríticas en ambientes con hidrocarburos a alta temperatura

Resumen

La corrosión a alta temperatura, tal como la carburación de materiales expuestos a una amplia variedad de ambientes agresivos, tiene especial importancia desde el punto de vista técnico e industrial. Estos ambientes incluyen productos de combustión, gases e hidrocarburos con bajo potencial de oxígeno y alto potencial de carbono. En las industrias de refinación y petroquímica, las aleaciones austeníticas y ferríticas se utilizan en tuberías de hornos. El rango de temperatura de exposición para aleaciones austeníticas está entre 800-1.100°C y para aleaciones ferríticas está entre 500-700°C, con actividades de carbono $a_c>1$ en algunos casos. En tuberías con ambas aleaciones, el proceso de carburación incluye deposición de carbón (coque) en el diámetro interno, absorción de carbono en la superficie del metal, difusión del carbono al interior de la aleación, precipitación y transformación de carburos a una profundidad creciente con el tiempo de servicio. La velocidad de crecimiento de la capa carburada interna es aproximadamente parabólica, controlada por la difusión del carbono y la precipitación de carburos. Las aleaciones ferríticas mostraron una carburación volumétrica uniforme, mientras que en las austeníticas se observó una carburación no uniforme a través de los granos y entre los límites de grano.

Palabras clave

Carburación. Corrosión a alta temperatura. Difusión. Aceros cromo-molibdeno. Aleaciones hierro-cromo-níquel.

1. INTRODUCTION

In industrial environments such as in oil refineries and petrochemical plants, engineering alloys such as Fe-Cr-Mo and Fe-Cr-Ni often come into contact with corrosive gases containing oxygen, sulfur, carbon, and nitrogen at a relatively low oxygen activities and high total pressure. The corrosive gases may participate in scale formation, or alternatively, may dissolve or diffuse internally

(*) Ecopetrol – Instituto Colombiano del Petróleo. Piedecuesta, Santander-Colombia.
(**) Ohio State University. Department of Materials Science and Engineering.

and react with alloy elements and precipitate as second phases within the grain or along the grain boundaries. Typical examples are thermal and steam cracking tubes in ethylene, propylene, synthesis gas production and fire heated tubes in crude oil and visbreaking furnaces[1-5].

Crude oil distillation and visbreaking are thermal cracking processes through which, at a moderate temperature of 500 to 700 °C, heavy hydrocarbon molecules are converted into lighter ones having a lower boiling point and greater economic value than the initial load[4]. The fire-heated tubes are Fe-Cr-Mo alloys (Fe-2 1/4Cr-1Mo, Fe-5Cr–1/2Mo, Fe-9Cr-1Mo). On the other hand, in ethylene steam crackers and syngas reformer furnaces, hydrocarbons and steam pass through tubes that are heated to temperatures above 900 °C in many cases exceeding 1100 °C. The alloys used in these furnaces are typically wrought stainless steels or Fe-Cr-Ni centrifugal cast alloys (HK, HP). In both cases, it is important to select the alloy composition or control the environment to minimize the damage produced by interactions with aggressive oxidants. These materials are selected because a scale rich in Cr_2O_3 is formed on the surface of these structural components which protects the material against high temperature corrosion. Strong oxidation, carburization, sulfidation or nitriding only occurs if the environment does not give to chromium oxide formation or if the protectivity of the scale is destroyed by other mechanisms[1-3].

Metals or alloys are generally susceptible to carburization when exposed to an environment containing CO, CH_4 or other hydrocarbon gases such as ethylene (C_2H_4) or propane (C_3H_8) at elevated temperatures. During thermal and steam cracking operation, carbon is deposited in the form of coke on the internal surfaces of the tubes. This has many deleterious effects. The efficiency of heat transfer is reduced and the metal skin temperature increased to maintain the process temperature. The presence of coke will eventually lead to carburization of the tubes when it is periodically removed by oxidation in water vapor and air. Carburization attack generally results in the formation of internal carbides that often cause the alloy to suffer embrittlement as well as other mechanical degradation[1-5], especially at low temperature.

2. THERMODYNAMICS

Petrochemical and refinery environments contain gas mixtures of CO, CO_2, H_2, H_2O, CH_4, H_xC_y (hydrocarbons), and organic compounds. The alloys are likely carburized if $(a_c)_{environment} > (a_c)_{alloy}$. This carburization can proceed by one of the following reactions:

$$CO + H_2 = C_{abs.} + H_2O \quad (1)$$

$$2CO = C_{abs.} + CO_2 \quad (2)$$

$$CH_4 = C_{abs.} + 2H_2 \quad (3)$$

In equilibrium, the carbon activity in the environment can be calculated by:

$$a_{C_{(1)}} = e^{-\Delta G_1^0/RT}\left(\frac{P_{CO}\cdot P_{H_2}}{P_{H_2O}}\right) = K_{(1)}\left(\frac{P_{CO}\cdot P_{H_2}}{P_{H_2O}}\right) \quad (4)$$

$$a_{C_{(2)}} = e^{-\Delta G_2^0/RT}\left(\frac{P_{CO}^2}{P_{CO_2}}\right) = K_{(2)}\left(\frac{P_{CO}^2}{P_{CO_2}}\right) \quad (5)$$

$$a_{C_{(3)}} = e^{-\Delta G_3^0/RT}\left(\frac{P_{CH_4}}{P_{H_2}^2}\right) = K_{(3)}\left(\frac{P_{CH_4}}{P_{H_2}^2}\right) = K_{(3)}\left(\frac{X_{CH_4}\,P^0}{X_{H_2}^2\,P}\right) \quad (6)$$

where,
a_C = Carbon activity
ΔG_i^0 = Standar Gibbs free energy reactioni
T = Absolute temperature
P_i = Reactant gases partial pressure
$K_{(1)}$ = Reaction equilibrium constant
P^0 = Standard pressure, 101.325 kPa (1 atm.)
P = Total system pressure
X_{CH_4} = CH_4 mole fraction
X_{H_2} = H_2 mole fraction

If the environment contains CH_4, the carbon activity of the environment will be dominated by the reaction (3) [1]. The figure 1 shows the

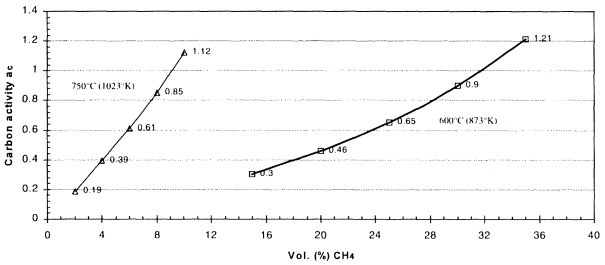

Figure 1. Variation of carbon activity with temperature and CH_4 composition in the mixture.

Figura 1. Variación de la actividad de carbono con la temperatura y la composición del CH_4 en la mezcla.

variation of carbon activity, (a_c), in the environment with temperature and gas composition, vol. (%), of a mixture H_2-CH_4 at 600 and 750 °C. For this reaction at all temperatures:

$$\Delta G_3^0 = 14669.52 - 1.987T\ (5.32\ \ln T - \\ - 0.00183T - 58832.41 / 2T^2 - 25.16) \quad (7)$$

In ferritic and austenitic alloys, ingress of carbon into the alloy results in the formation of chromium carbides, principally. There are three forms of chromium carbides: $Cr_{23}C_6$, Cr_7C_3, and Cr_3C_2. During carburization, a stability diagram such as the one shown in figure 2 can best describe the relative stability of these carbides. At very low oxygen partial pressure and low carbon activity in the alloy, the most stable carbide is $Cr_{23}C_6$. Considering the following equilibrium[7 and 8]:

$$\frac{23}{6}\,Cr_{(S)} + C_{(g)} = \frac{1}{6}\,Cr_{23}C_{6\,(S)} \quad (8)$$

$$\Delta G_f^0 = -RT \ln\left(\frac{a_{Cr_{23}C_6}^{1/6}}{a_C \cdot a_{Cr}^{23/6}}\right) \quad (9)$$

Where $a_{Cr_{23}C_6}$ the activity of the solid carbide precipitated, is assumed to be unity. Rearranging the equation (9), it becomes:

$$(a_C)_{alloy} = e^{\Delta G_f^0 / RT}\left(\frac{1}{a_{Cr}^{23/6}}\right) \quad (10)$$

In this case:

ΔG_f^0 = Standard Gibbs energy of carbide formation.
a_{Cr} = Chromium activity in the alloy.

The standar Gibbs energies of formation of some carbides are showed in figure 3. For all temperatures,

$$\Delta G_f^0 = 16380 + 1.54T \quad (11)$$

and

$$a_{Cr} = \gamma_{Cr} \cdot N_{Cr} \quad (12)$$

Here:
γ_{Cr} = Chromium activity coefficient
N_{Cr} = Molar fraction of chromium

For the system Fe-Cr-Mo [10]

$$\text{Ln}\ \gamma_{Cr} = \alpha\ (N_{Fe})^2 \quad (13)$$

With
α = A constant independent of concentration and

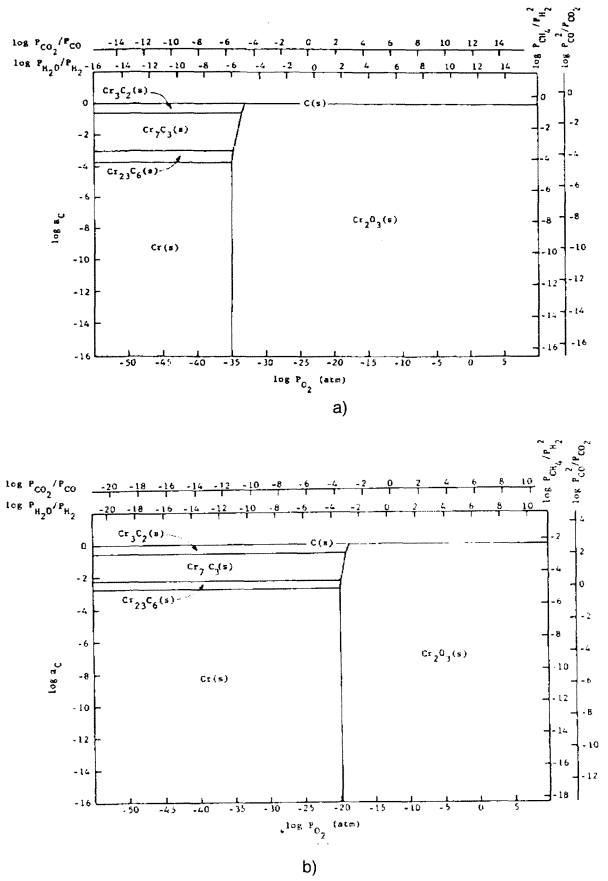

Figure 2. Phase stability diagrams of Cr-C-O system at (a) 620 °C and (b) 1090 °C [6].

Figura 2. Diagrama de estabilidad de fases para el sistema Cr-C-O. a) a 620 °C y b) a 1090 °C [6].

inversely related with temperature. It has a value of 2 at 560 °C.
N_{Fe} = Iron molar fraction in the alloy, equal to 0.8821 and calculated from table I.

With these values, $\gamma_{Cr} = 4.74$; $a_{Cr} = 0.4355$ and $(a_C)_{alloy} = 0.002$. Similar calculations are possible for the system Fe-Cr-Ni.

3. FIELD CARBURIZATION

The main object of this paper is to compare the morphological differences in carburization occurred in austenitic and ferritic alloys exposed for a long time in environments with carbon activity over one in many cases. The carbon activity inside the alloys is too low and thermodynamic calculations show a high potential for carbon diffusivity.

Carburization proceeds both along grain boundaries (grain boundary carburization) as well as within the grains (bulk carburization). Samples

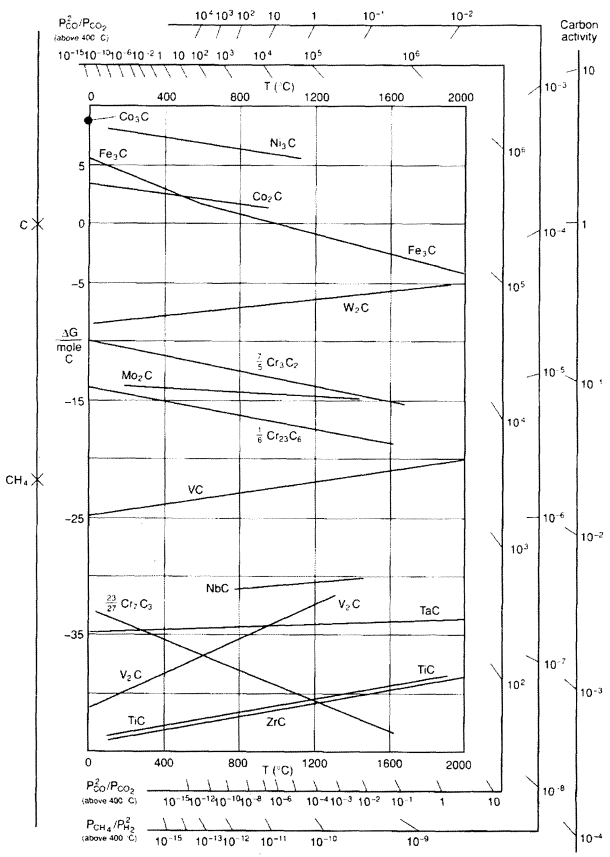

Figure 3. Standard free energies of formation for some carbides[7].

Figura 3. Energía libre estándar de formación para algunos carburos [7].

extracted from tubes of fired furnaces, visbreaking and pyrolysis furnaces, show this difference. In the first case, in a sample of ferritic alloy 9Cr-1Mo extracted from a tube closed to the outlet of the radiation zone shows the evident bulk carburization through all the cross section along the inside diameter. This tube had 102000 h of continuous exposition at 600 °C, average. In the second example, a the tube of alloy HP-40 extracted from a coil of the radiation zone of the furnace had 88000 h of continuous exposition over 900 °C, but in this case carburization only occurred along the austenitic grain boundary, see figure 4(a) for ferritic alloy and figure 4(b) for an austenitic alloy. This performance suggests two different mechanisms of carburization in this particular application of alloys in the oil refinery and the petrochemical industry.

Although the alloy 9Cr-1Mo had an oxide layer over the internal surface, the carburization was homogeneous along the internal diameter. Conversely, the presence of a pre-existing oxide film over the internal surface in the alloy HK-40, formed in air before exposure to the carburization environment, reduced or inhibited carburization. Porosity, cracks, spallation and possible reduction of chromium oxides to carbides can occur and the underlying metal matrix will consequently be exposed to the carburizing environment[11].

4. CONCLUSIONS

In industrial visbreaking and pyrolysis furnaces, the carbon environment activity is hardly dependent

Table I. Composition of 9Cr-1Mo modified ferritic steel and calculation of iron molar fraction

Tabla I. Composición química del acero ferrítico Fe-9Cr-1Mo modificado y cálculo de la fracción molar del hierro

Element	Concentration Wt (%)	Molecular weight (g/g mol)	Number of moles	Molar fraction N
C	0.094	12	0.007 834	0.004 34
Mn	0.431	55	0.007 836	
P	0.016	31	0.000 516	
S	0.006	32	0.000 187	
Si	0.370	28	0.013 214	
Cu	0.020	64	0.000 312	
Ti	0.009	48	0.000 187	
Co	0.019	59	0.000 322	
Sn	0.006	119	0.000 050	
Cr	8.618	52	0.165 731	0.091 90
Mo	0.965	96	0.010 052	
V	0.204	51	0.004 000	
Ni	0.077	59	0.001 305	
Al	0.029	27	0.001 074	
Nb	0.086	93	0.000 924	
Fe	89.104	56	1.591 143	0.882 10
		Total moles	1.804 070	

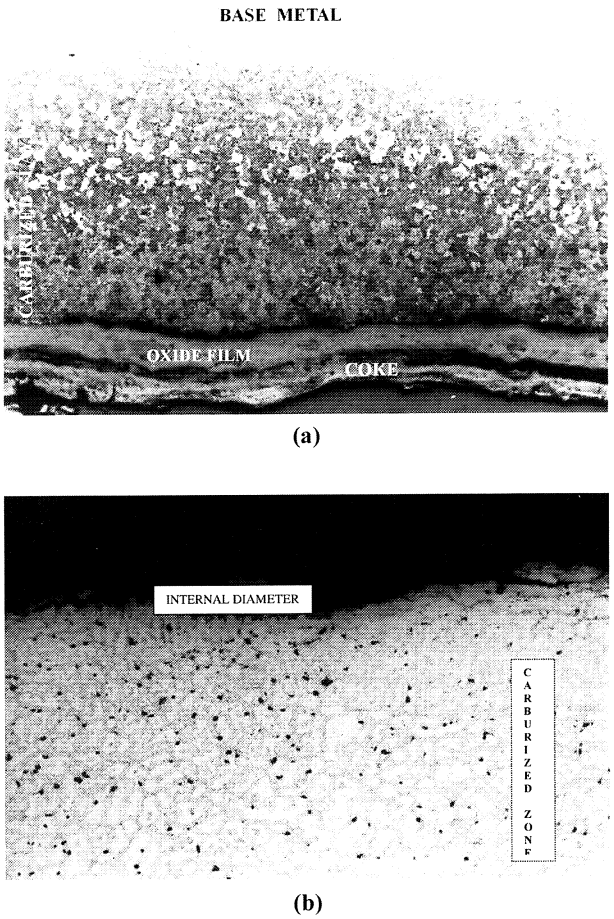

Figure 4. (a) Cross section of a steel 9Cr-1Mo carburized in the radiation zone of a visbreaking furnace after 102 000 h of continuous exposition 100X. (b) View of the internal cross section of austenitic steel HP-40 used in the production of ethylene 100X.

Figura 4. (a) Sección transversal carburada del acero 9Cr-1Mo extraída de la zona de radiación del horno de viscorreducción después de 102.000 h de exposición continua. 100X. (b) Vista de la sección transversal interna del acero austenítico HP-40 utilizado en los hornos de producción de etileno. 100X.

of temperature and blend gas composition. At low temperature the CH_4 concentration in the mixture H_2-CH_4 is too high resulting in a high carbon potential.

Bulk carbon diffusion is the main mechanism of carburization in ferritic alloys Fe-9Cr-1Mo observed in samples extracted from visbreaking fired furnace tubes. A mathematical model similar to the unidirectional internal oxidation that considers the interaction between carbon and active elements is applicable for describing this phenomenon.

Boundary grain precipitation is the main mechanism of carburization in austenitic Fe-Ni-Cr (HP-40) alloys observed for samples extracted from ethylene furnace tubes. In this case the simple unidirectional mathematical model used for explaining internal oxidation or describing carburization needs a different and additional arrangement. In this particular case, was seen internal carburization only in areas where the oxide film was absent.

The different behavior mechanism for ferritic and austenitic alloys involves several factors: for ferrite, carbon solubility is much less but carbon diffusivity is much higher; chromium diffusivity is much higher. For austenite, carbon solubility is high, but carbon diffusivity is low, and chromium diffusivity is low. The grain boundary precipitation for austenitic alloys does not mean that grain boundary carbon diffusion was important, because carbon is quite soluble in austenite and does not need the grain boundary for diffusion. Rather, probably the $Cr_{23}C_6$ lattice does not match well to the austenite lattice (perhaps better to the ferrite lattice). Therefore, the precipitation fits better in the austenite grain boundary than in the austenite bulk. Besides precipitation in a lattice also requires lattice diffusion of solvent atoms. This is faster in ferrite, but in austenite, grain boundary diffusion for iron may be needed.

Acknowledgements

This analysis was carried out in the Ecopetrol's Materials Technology, ICP-KTC Laboratories. Special thanks go to W. Afanador and Carmen A. Dorado for their technical contributions to the work.

REFERENCES

[1] G.Y. LAI, *High Temp. Corros. Eng. Alloys* (1990) 47- 72.
[2] P. KOFSTAD, *High Temp. Corros.* (1988) 511-536.
[3] H.J. GRABKE, *Carburization* 52 (1998) 194.
[4] A. SERNA, *Technol. Law Insur.* 2 (1997) 85-93.
[5] S. FORSETH, Ph.D. Thesis, Dept. of Chemistry, Oslo, 1995.
[6] P. HEMMINGS and R. PERKINS, *Thermodynamic Phase Stability Diagrams for the Analysis of Corrosion Reactions in Coal Gasification/Combustion Atmospheres*, EPRI, USA, 1997, pp. 26-28.
[7] J. HUCINSKA, *Eurocorr'97*, Event Nº 208, Vol. II, EFC, Norway, 1997, pp. 23-28.
[8] J.A. COLWELL and R.A. RAPP, *Metall. Trans.* A. 17A, (1986) 1065-1074.
[9] S.R. SHATYNSKI, *Oxid. Met.* 13 (1979) 105.
[10] M. SMALL and E. RYBA, *Metall. Trans.* A 12A (1981) 1389-1396.
[11] J. CHU and A. RAHMEL, *Oxid. Met.* 15 (1981) 331-337.